

A mean field approach for computing solid-liquid surface tension for nanoscale interfaces

Chi-cheng Chiu,¹ R. J. K. Udayana Ranatunga,¹ David Torres Flores,² D. Vladimir Pérez,³ Preston B. Moore,³ Wataru Shinoda,⁴ and Steven O. Nielsen^{1,a)}

¹*Department of Chemistry, The University of Texas at Dallas, 800 West Campbell Road, Richardson, Texas 75080, USA*

²*Division de Ciencias Exactas, Universidad de Guanajuato, Campus Guanajuato, Callejon Jalisco, Valenciana, Guanajuato 36240 Gto., Mexico*

³*Department of Chemistry and Biochemistry, University of the Sciences in Philadelphia, Philadelphia, Pennsylvania 19104, USA*

⁴*Research Institute for Computational Sciences, National Institute of Advanced Industrial Science and Technology (AIST), Central 2, 1-1-1, Umezono, Tsukuba, Ibaraki 305-8568, Japan*

(Received 15 October 2009; accepted 13 January 2010; published online 4 February 2010)

The physical properties of a liquid in contact with a solid are largely determined by the solid-liquid surface tension. This is especially true for nanoscale systems with high surface area to volume ratios. While experimental techniques can only measure surface tension indirectly for nanoscale systems, computer simulations offer the possibility of a direct evaluation of solid-liquid surface tension although reliable methods are still under development. Here we show that using a mean field approach yields great physical insight into the calculation of surface tension and into the precise relationship between surface tension and excess solvation free energy per unit surface area for nanoscale interfaces. Previous simulation studies of nanoscale interfaces measure either excess solvation free energy or surface tension, but these two quantities are only equal for macroscopic interfaces. We model the solid as a continuum of uniform density in analogy to Hamaker's treatment of colloidal particles. As a result, the Hamiltonian of the system is imbued with parametric dependence on the size of the solid object through the integration limits for the solid-liquid interaction energy. Since the solid-liquid surface area is a function of the size of the solid, and the surface tension is the derivative of the system free energy with respect to this surface area, we obtain a simple expression for the surface tension of an interface of arbitrary shape. We illustrate our method by modeling a thin nanoribbon and a solid spherical nanoparticle. Although the calculation of solid-liquid surface tension is a demanding task, the method presented herein offers new insight into the problem, and may prove useful in opening new avenues of investigation. © 2010 American Institute of Physics. [doi:10.1063/1.3308625]

I. INTRODUCTION

Most of the physical properties of a liquid in contact with a solid depend on the solid-liquid surface tension. Development of methods that allow for the determination of solid-liquid surface tension using molecular simulation is still an ongoing task.¹ Reliable simulation methods are of crucial importance because experimental techniques cannot directly measure surface tension at the nanoscale (e.g., for small colloids); instead experimental measurements of contact angles are used in conjunction with a theoretical framework to estimate the surface tension.² However, assignment of surface tension from contact angle data for nanoscale interfaces is a controversial and unresolved issue.^{3,4}

The calculation of solid-liquid surface tension is undoubtedly a challenging task. While we make no pretension here to fully resolve all of the difficulties, we believe that the method to be described offers new insight into the problem,

and may prove useful in opening up new lines of attack, for example, when combined with the recent method of Leroy *et al.*¹

In most simulation studies the surface tension has been determined by using the virial expression; for a planar interface this involves the difference of pressure tensor components normal and tangential to the interface, $\gamma = L_{\perp}(P_{\parallel} - P_{\perp})$, where L_{\perp} denotes the simulation unit cell length perpendicular to the interface.^{5,6} Salomons and Mareschal⁷ rigorously proved that the virial expression is equivalent to the thermodynamic definition of surface tension $\gamma = (\partial F / \partial A)_{NVT}$, where F is the Helmholtz free energy and A is the surface area of the interface. They went on to formulate a novel method based directly on the thermodynamic definition in which the free energy of a small isothermal, volume-conserving deformation of the system which increased the interfacial area was computed. Furthermore, this alternative method was suggested as being applicable to geometries other than planar.

In a similar spirit to Salomons and Mareschal, we introduce here a novel method to compute the surface tension of a planar interface based directly on the thermodynamic defi-

^{a)}Electronic mail: steven.nielsen@utdallas.edu.

dition. Importantly, our method also applies to curved interfaces and reveals the exact relationship between the surface tension and the excess solvation free energy per unit surface area. These quantities are not equivalent for nanoscale interfaces, yet most simulation studies of nanoscale interfaces have measured excess solvation free energy and not surface tension.⁸⁻¹⁴ We present below the formulation for planar interfaces of finite width and spherical interfaces of positive curvature. Other geometries, including interfaces of negative curvature, follow in a straightforward manner but are beyond the scope of the present study.

The methods we present here rely on a mean field treatment of the solid objects. Such an approach has a long history in science. For example, Hamaker based his 1937 paper on the van der Waals attraction between solid spherical particles on such a treatment,¹⁵ and this treatment underlies the Derjaguin, Landau, Verwey, and Overbeek theory of colloids. In terms of computer simulations, such approaches for calculating surface tension go back at least to 1976 when Miyazaki *et al.* computed the free energy of converting a solid-liquid interface to a liquid-vapor interface by sliding a solid wall outwards and integrating the derivative of the free energy with respect to the position of the wall.¹⁶ The advantages to using such a mean field approach are fourfold. First, it allows us to get rid of inessential details of real materials which might otherwise obscure the universal features of the curvature and nanoscale size phenomena in question. Second, it allows us to use ideal defect-free substrate surfaces, thus eliminating a lot of practical complications. Third, in contrast to experiments, it allows us to easily vary parameters such as the solid-liquid interaction strength and monitor the resulting surface tensions. Fourth, it allows us to develop analytic expressions which reveal the underlying physics and the relationship between surface tension and excess solvation free energy.

We begin by casting the thermodynamic expression for surface tension in a form amenable to a mean field treatment. Based on this formulation, we outline how one would compute the solid-liquid surface tension without using the mean field description in order to illustrate the nature of the full problem. We then proceed to use a mean field description for the solid and present in detail the treatment of planar and spherical interfaces. Our analysis shows that the surface tension and the excess solvation free energy per unit surface area of a nanoscale interface are in general inequivalent; their precise relationship is derived for each of the interfaces we consider and their inequivalence is validated with extensive molecular dynamics (MD) simulation data.

II. THERMODYNAMIC DEFINITION OF SOLID-LIQUID SURFACE TENSION

The surface tension, γ , of an interface is defined in thermodynamics as

$$\gamma = \left(\frac{\partial F}{\partial A} \right)_{\text{NVT}} = \left(\frac{\partial G}{\partial A} \right)_{\text{NPT}}, \quad (1)$$

where F is the Helmholtz free energy of the system, G is the Gibbs free energy, and A is the surface area of the interface.

Consider an interface between a liquid and a solid. Let us assign a size a with units of length to the solid object in some manner, and use the chain rule to write (with an equivalent formula for F)

$$\frac{\partial G}{\partial A} = \frac{\partial G}{\partial a} \frac{da}{dA} = \frac{\partial G}{\partial a} \left(\frac{dA(a)}{da} \right)^{-1}. \quad (2)$$

This formulation accommodates a range of solids, from spherical where $A(a) = 4\pi a^2$ with a the radius, to truncated icosahedral where $A(a) = 3a^2(10\sqrt{3} + \sqrt{5}\sqrt{5+2\sqrt{5}})$ with a the edge length, to any other shape for which the surface area can be written as a function of a single parameter.

III. MEAN FIELD MACHINERY

We will use a mean field approach in Secs. VI and VII which imbues the solid-liquid intermolecular potential energy with parametric dependence on a . In this section we wish to explore the consequences of such an approach on Eq. (2). As pointed out by Onsager, parameters which appear in the potential of the intermolecular interactions have essentially the same status as the parameters of external force and may be manipulated in the same manner.¹⁷ Hence, we may write

$$\frac{\partial G}{\partial a} = \frac{\partial}{\partial a} \left(-\frac{1}{\beta} \ln Q \right) = \frac{1}{Q} \int dx \frac{\partial U}{\partial a} e^{-\beta H} = \left\langle \frac{\partial U}{\partial a} \right\rangle, \quad (3)$$

where Q is the canonical partition function, x represents all the particle coordinates and momenta, U is the potential energy of the system, and the angle brackets are understood to be evaluated in the canonical ensemble. Likewise, we have

$$\begin{aligned} \frac{\partial G}{\partial a} &= \frac{\partial}{\partial a} \left(-\frac{1}{\beta} \ln \Delta \right) \\ &= \frac{1}{\Delta} \int_0^\infty dV \int dx \left(\frac{\partial U}{\partial a} + P \frac{\partial V}{\partial a} \right) e^{-\beta H} e^{-\beta PV} \\ &= \left\langle \frac{\partial U}{\partial a} \right\rangle + P \left\langle \frac{\partial V}{\partial a} \right\rangle, \end{aligned} \quad (4)$$

where Δ is the isothermal-isobaric partition function and the angle brackets are understood to be evaluated in the isothermal-isobaric ensemble. The PV term is usually negligibly small⁸ but can easily be computed either by simply monitoring the unit cell size in MD simulations for different values of a (keeping the number of liquid particles fixed), or by assuming the liquid is incompressible in which case the known dependence of the solid volume on the size a can be used. The mean field approach will allow us to compute $\langle \partial U / \partial a \rangle$ from a single equilibrium MD simulation. This is our machinery: we have turned $\partial G / \partial a$ into an expression which can be easily computed from an equilibrium MD run which through Eqs. (1) and (2) gives us the surface tension.

IV. HOW TO CALCULATE SOLID-LIQUID SURFACE TENSION WITHOUT THE MEAN FIELD APPROACH

The advantage of using the mean field approach can be illustrated by the problem of *not* using it. In this context, we

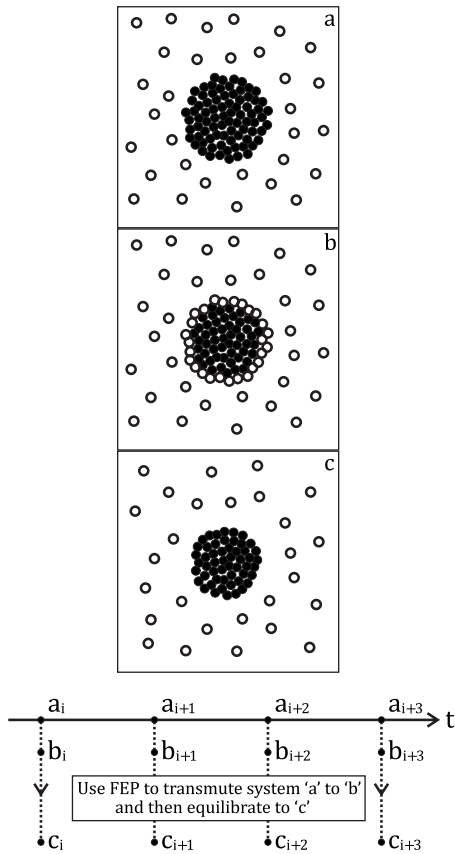


FIG. 1. Schematic plan to measure the surface tension of a solid-liquid interface with an explicit representation of the solid. At various times i during an equilibrium MD simulation (panel a), the interfacial area is reduced using alchemical free energy perturbation techniques (panel b), and then equilibrated (panel c). See the text for details.

wish to conduct a thought experiment to directly compute the surface tension of a solid-liquid interface using MD simulations without any idealizations. From Eqs. (1)–(3) we are required to evaluate $\langle \partial U / \partial a \rangle$. We assume the ergodic hypothesis and replace the ensemble average with a time average,¹⁸

$$\left\langle \frac{\partial U}{\partial a} \right\rangle = \frac{1}{T} \sum_{t_i=1}^T \frac{\partial U_{t_i}}{\partial a}. \quad (5)$$

Consider a particular time t_i , sketched in Fig. 1(a). At this stage of the argument, since we have not yet replaced the solid with a mean field, we can evaluate $\partial U / \partial a$ by finite difference as follows. Assume that the solid particle in Fig. 1(a) is of characteristic size a . As shown in Fig. 1(b), let us replace the solid atoms in the range $(a - \Delta a, a)$, measured from the center of the solid, with liquid particles using, for example, an alchemical free energy perturbation approach.¹⁹ These liquid particles are initially out of equilibrium because, among other reasons, they have the wrong local density. We can run a short MD simulation to let them diffuse and come to equilibrium with the existing fluid phase, shown in Fig. 1(c). Then, we can form $\partial U / \partial a$ by finite difference

$$\frac{\partial U}{\partial a} \approx \frac{U^{(c)} - U^{(a)}}{\Delta a}, \quad (6)$$

where the superscripts (a) and (c) refer to the systems in Figs. 1(a) and 1(c), respectively.

However, there is a numerical problem with this calculation because of how systems (a) and (c) differ from one another. Clearly the solid-liquid interface is different since we have explicitly changed it (e.g., it has a different curvature). Unfortunately, the noninterfacial solid particles and the noninterfacial liquid particles have evolved through various mechanisms such as librations and diffusion. Ultimately such fluctuations in the noninterfacial parts of the system cancel out in the equilibrium average of Eq. (5) and hence do not contribute to γ . However, their contribution to the individual measurements on the right hand side of Eq. (6) dominates over the interfacial contribution simply due to the respective number of particles involved; the former (bulk) region is three dimensional and the latter (interfacial) region is two dimensional. In other words, the signal is swamped by the noise. The mean field approach, as demonstrated in Secs. VI and VII, eliminates these fluctuations or, in other words, removes the noise from the signal and allows an accurate estimation of $\langle \partial U / \partial a \rangle$.

V. LIQUID FORCE FIELD AND SIMULATION DETAILS

We used two different liquid models to illustrate the general applicability of our mean field method: the Lennard-Jones (LJ) model and a coarse grain water model. For the LJ model, the potential energy between liquid particles is given by $u_{ll}(r) = 4\epsilon_{ll}[(\sigma_{ll}/r)^{12} - (\sigma_{ll}/r)^6]$. Reduced units are used for all reported quantities where the unit of length is σ_{ll} , the unit of energy is ϵ_{ll} , the unit of mass is the particle mass, and the unit of temperature is ϵ_{ll}/k_B where k_B is Boltzmann's constant. We used a temperature of $T = 0.75$ and a time step of $\tau = 5 \times 10^{-4}$.^{20,21} The interaction between LJ particles is truncated at $3\sigma_{ll}$ and no long-range corrections are included for either the energy or pressure. For the interaction between the solid strip and the liquid, we take $\sigma_{sl} = \sigma_{ll}$ and measure the solid-liquid interaction energy ϵ in units of ϵ_{ll} (see Sec. VI).

The interaction between water molecules is modeled using the recent coarse grain force field of Shinoda.^{22,23} This model reproduces the experimental liquid-vapor surface tension which is the most importance physical property of the solvent related to our study. The potential energy between water sites is given by $u_{ll}(r) = 3(3)^{1/2}\epsilon_{ll}/2[(\sigma_{ll}/r)^{12} - (\sigma_{ll}/r)^4]$, where r is the distance between the molecules and where $\epsilon_{ll} = 0.895$ kcal/mol and $\sigma_{ll} = 4.37$ Å. We used a temperature of 303 K and a time step of 3 fs for the water-solid and short-ranged water-water interactions and 30 fs for long-ranged ($r > 6$ Å) water-water interactions. The water-water interaction is truncated at 15 Å and no long-range energy or pressure corrections are included.

The MD simulations were performed using the CM3D and MPDYN MD packages.^{24,25} All simulations were run under the isothermal-isobaric ensemble at the specified temperature and atmospheric pressure. For each of the 10 values of ϵ shown in Fig. 2, 3500 liquid particles were simulated for

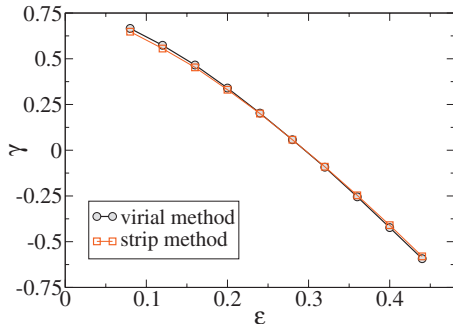


FIG. 2. Surface tension of a planar interface computed using the strip method (for a strip width of $2a=8$) vs the virial (pressure tensor) method as a function of the solid-liquid interaction strength ϵ . All quantities are expressed in dimensionless units.

1×10^7 time steps for the virial method and 2.5×10^6 time steps for the strip method. For the 16 values of a used in Fig. 3, 3500 liquid particles were simulated for 5×10^6 time steps. For each of the nine values of ϵ shown in Fig. 5, we performed 30 equilibrium simulations for 10 ns each with spheres of radii 1, 2, ..., 30 Å in unit cells with between 5000 and 30 000 water sites. The solid objects are treated as follows: the planar strip can be viewed as being infinitely long and is hence assigned an infinite mass; on the other hand the solid sphere is finite in extent and is assigned a mass proportional to its volume and is thus displaced during the MD simulations according to the forces it experiences from the liquid particles.

VI. PLANAR STRIP

Consider a planar strip of solid material, for example, a graphene nanoribbon, characterized by a width $2a$; assume for convenience the strip is in the x - y plane, oriented along the x -axis. In the mean field approach, we replace the lattice sites which constitute the solid with a continuum in analogy to Hamaker's treatment.¹⁵ To derive the resulting solid-liquid interaction potential, we suppose that the strip has an atomic number area density $\rho=1.6$ (expressed as the number of atoms per unit area in dimensionless units; see Sec. V), and that the van der Waals interaction energy between one of these atoms and a liquid atom is given by $u_{sl}(d) = 4\epsilon[(\sigma_{sl}/d)^{12} - (\sigma_{sl}/d)^6]$, where d is the distance between the

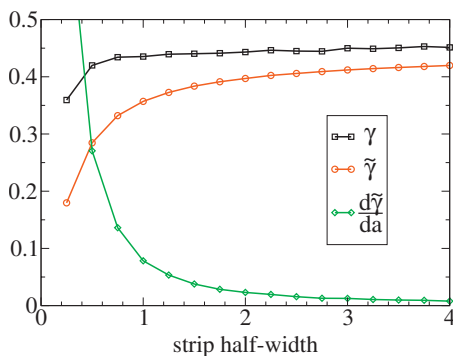


FIG. 3. Variation in the solid-liquid surface tension γ , excess free energy per unit surface area $\tilde{\gamma}$, and its derivative $d\tilde{\gamma}/da$ with the strip half-width a for a solid-liquid interaction strength of $\epsilon=0.16$. All quantities are expressed in dimensionless units.

solid and liquid atoms, ϵ is the tunable solid-liquid interaction strength, and $\sigma_{sl}=\sigma_{ll}$. The potential energy between a liquid atom and the entire solid object is then obtained in the mean field model by integrating over the continuum solid, $U = \int_A \rho u_{sl} dA$ where A is the area of the solid strip. For purposes of integration, we can without loss of generality place the liquid atom at position $(0, y_0, z_0)$ to obtain

$$U(y_0, z_0; a) = 4\epsilon\rho \int_{-a}^a dy \int_{-\infty}^{\infty} dx \left[\frac{\sigma_{sl}^{12}}{(x^2 + (y - y_0)^2 + z_0^2)^{12/2}} - \frac{\sigma_{sl}^6}{(x^2 + (y - y_0)^2 + z_0^2)^{6/2}} \right] \\ = \epsilon\rho \int_{-a}^a dy \left[\frac{63\pi\sigma_{sl}^{12}}{64((y - y_0)^2 + z_0^2)^{11/2}} - \frac{3\pi\sigma_{sl}^6}{2((y - y_0)^2 + z_0^2)^{5/2}} \right]. \quad (7)$$

Notice that ϵ and ρ appear simply as linear factors in Eq. (7); choosing a different value for ρ yields the same potential $U(y_0, z_0; a)$ if ϵ is rescaled appropriately. The y integral can be performed to arrive at an analytic expression for $U(y_0, z_0; a)$ but the resulting expression is too long to include here; analytic expressions also exist for the force $(0, -\partial U/\partial y_0, -\partial U/\partial z_0)$ on the liquid particle. The derivative needed to access the surface tension, $\partial U/\partial a$, is simply

$$\frac{\partial U}{\partial a} = \frac{63\pi\epsilon\rho\sigma_{sl}^{12}}{64} \left[\frac{1}{((a + y_0)^2 + z_0^2)^{11/2}} + \frac{1}{((a - y_0)^2 + z_0^2)^{11/2}} \right] \\ - \frac{3\pi\epsilon\rho\sigma_{sl}^6}{2} \left[\frac{1}{((a + y_0)^2 + z_0^2)^{5/2}} + \frac{1}{((a - y_0)^2 + z_0^2)^{5/2}} \right]. \quad (8)$$

The strip area is given by

$$A(a) = 2(a + \delta)L_x, \quad (9)$$

where L_x is the unit cell dimension in the x -direction and the parameter δ accommodates any particular choice of the Gibbs dividing surface. From Eqs. (2) and (4) we may write the surface tension as

$$\gamma = (2L_x)^{-1} \left\langle \sum_i \frac{\partial U_i}{\partial a} \right\rangle \Rightarrow \frac{\partial G}{\partial a} = 2L_x\gamma, \quad (10)$$

where i indices the liquid particles. The strip surface tension data for a strip width of $2a=8$ is compared in Fig. 2 to the surface tension of an infinitely extended planar interface computed using the virial expression. The infinitely extended interface is described by taking $a \rightarrow \infty$, yielding

$$U(z_0) = 4\pi\epsilon\rho \left[\frac{4\sigma_{sl}^{12}}{5z_0^{10}} - \frac{2\sigma_{sl}^6}{z_0^4} \right]. \quad (11)$$

The agreement is seen to be quantitative because the strip is wide enough to essentially be free of finite size effects.

Through

$$G(a) = \int_0^a \frac{\partial G}{\partial w} dw, \quad (12)$$

we may identify $G(a)$ with the excess solvation free energy of the solid object where the right hand side of Eq. (12) is understood to be evaluated by thermodynamic integration; w here is a dummy integration variable representing the strip half-width. $G(a)$ can be thought of as the free energy cost of growing the solid object in the solvent from a vanishingly small size to size a , or equivalently, as the free energy cost of transferring the planar strip of half-width a from an ideal gas reference state into the solvent.

We define the excess solvation free energy per unit surface area using Eq. (9) by

$$\tilde{\gamma} = G(a)/A(a) = [2(a + \delta)L_x]^{-1}G(a), \quad (13)$$

and denote it with $\tilde{\gamma}$ to distinguish it from the surface tension γ . From Eq. (13) we have

$$\frac{\partial G}{\partial a} = 2L_x\tilde{\gamma} + 2(a + \delta)L_x\frac{\partial\tilde{\gamma}}{\partial a}. \quad (14)$$

Combining this with Eq. (10) gives

$$\gamma = \tilde{\gamma} + (a + \delta)\frac{\partial\tilde{\gamma}}{\partial a}, \quad (15)$$

which is a differential equation relating γ and $\tilde{\gamma}$. The surface tension and the solvation free energy per unit surface area are seen to be different if $\tilde{\gamma}$ depends on a . To simplify the analysis of Eq. (15), let us take $\delta=0$ and assume that L_x is independent of a , which could be realized by adjusting the number of liquid particles between simulations to compensate for the different planar strip excluded volumes. We then see that

$$\frac{\partial\tilde{\gamma}}{\partial a} = \frac{1}{a^2} \left(a\gamma - \int_0^a \gamma dw \right), \quad (16)$$

from which it is clear that $\partial\tilde{\gamma}/\partial a$ is nonzero if γ varies with a over some range of a -values. Specifically, we see from Eq. (16) that the difference between γ and $\tilde{\gamma}$ as per Eq. (15) depends on how quickly γ reaches its plateau value; the data in Fig. 3 shows that this happens very quickly. Nonetheless, γ and $\tilde{\gamma}$ are clearly distinguishable for all strip widths considered in Fig. 3. Moreover, a careful examination of the data shows that the $a=4$ value of γ is ever so slightly different from its $a \rightarrow \infty$ extrapolation, which explains the very small but systematic discrepancy between the two curves of Fig. 2.

VII. SOLID SPHERE

Consider a solid sphere of radius a and suppose that the van der Waals interaction energy between a lattice site in the solid and a liquid site is given by $u_{sl}(d) = 27\epsilon/4[(\sigma_{sl}/d)^9 - (\sigma_{sl}/d)^6]$, where d is the distance between the sites, ϵ is the tunable solid-liquid interaction strength, and $\sigma_{sl} = 4.0 \text{ \AA}$. The LJ 9-6 functional form used here is typical of coarse grain force fields.^{22,23}

The potential energy between a single liquid site and the entire solid sphere is obtained in the mean field model by integrating over the continuum solid, $U = \int_V \rho u_{sl} dV$ where V

is the volume of the sphere and ρ is the number density of lattice sites in the solid sphere. For purposes of integration, we can without loss of generality place the solid at the origin and the liquid site at $(0, 0, R)$. An interaction site in the solid is located at position $(r \sin \phi \cos \theta, r \sin \phi \sin \theta, r \cos \phi)$, so that the integral can be written explicitly as

$$U = \int_0^a \int_0^{2\pi} \int_0^\pi r^2 \sin \phi \rho u_{sl}(\xi) d\phi d\theta dr, \quad (17)$$

where a is the sphere radius, R is the distance between the sphere center and a liquid molecule, and $\xi^2 = r^2 - 2rR \cos \phi + R^2$.

The integration can be performed analytically, yielding

$$U(R; a) = \frac{9\pi\epsilon\rho\sigma_{sl}^9 a^3 (3a^4 + 42a^2 R^2 + 35R^4)}{35R(R^2 - a^2)^6} - \frac{9\pi\epsilon\rho\sigma_{sl}^6 a^3}{(R^2 - a^2)^3}. \quad (18)$$

We use $\rho = 3.76 \times 10^{-2} \text{ \AA}^{-3}$. Once again, notice that ϵ and ρ appear simply as linear factors in Eq. (18); choosing a different value for ρ yields the same potential $U(R; a)$ if ϵ is rescaled appropriately.

The interfacial area of the sphere is given by

$$A(a) = 4\pi(a + \delta)^2, \quad (19)$$

where the parameter δ accommodates any particular choice of the Gibbs dividing surface. From Eqs. (2) and (4), we may write

$$\gamma = [8\pi(a + \delta)]^{-1} \left\langle \sum_i \frac{\partial U_i}{\partial a} \right\rangle \Rightarrow \frac{\partial G}{\partial a} = 8\pi(a + \delta)\gamma \quad (20)$$

where i indices the liquid particles. We define the excess solvation free energy per unit surface area using Eq. (19) by

$$\tilde{\gamma} = G(a)/A(a) = [4\pi(a + \delta)^2]^{-1}G(a), \quad (21)$$

and denote it with $\tilde{\gamma}$ to distinguish it from the surface tension γ , where $G(a)$ is the excess solvation free energy of the solid sphere defined in an analogous manner to Eq. (12). From Eq. (21) we have

$$\frac{\partial G}{\partial a} = 8\pi(a + \delta)\tilde{\gamma} + 4\pi(a + \delta)^2 \frac{\partial\tilde{\gamma}}{\partial a}. \quad (22)$$

Combining this with Eq. (20) gives

$$\gamma = \tilde{\gamma} + \frac{a + \delta}{2} \frac{\partial\tilde{\gamma}}{\partial a}, \quad (23)$$

which is a differential equation relating γ and $\tilde{\gamma}$. Our formalism makes this relationship explicit, which is one of its great strengths. Clearly $\lim_{a \rightarrow \infty} \tilde{\gamma} = \lim_{a \rightarrow \infty} \gamma = \gamma_\infty$, which corresponds to the surface tension of a planar solid-liquid interface.²⁶ In Fig. 4 we explicitly compare γ and $\tilde{\gamma}$ for three different values of the solid-liquid interaction strength ϵ and two different choices of the dividing surface δ . The asymptotic value γ_∞ is determined by the strength of the solid-liquid interaction energy ϵ . There is no restriction on the sign of γ_∞ as long as the liquid-vapor surface tension is positive.²⁷

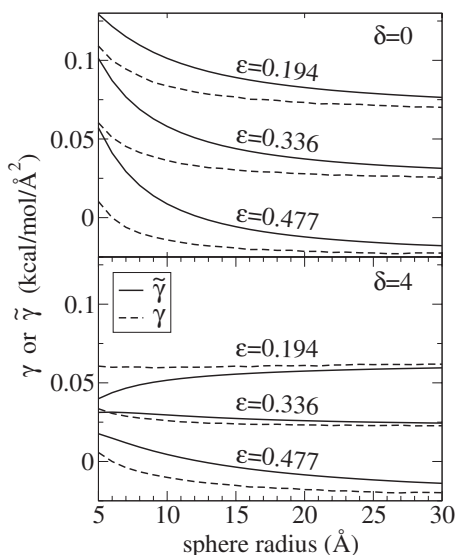


FIG. 4. For a spherical solid-liquid interface, the excess free energy per unit surface area $\tilde{\gamma}$ and the surface tension γ are plotted for three different values of the solid-liquid interaction strength ϵ (kcal/mol) and two different values of the dividing surface δ (Å). See Eqs. (20) and (21) and the accompanying text for details.

Let us express $\tilde{\gamma}$ in inverse powers of the sphere radius a

$$\tilde{\gamma} = \gamma_{\infty} + c_1 a^{-1} + c_2 a^{-2} + \dots, \quad (24)$$

Up to second order, Eq. (23) yields

$$\gamma = \gamma_{\infty} + \frac{c_1}{2a} - \frac{\delta c_1}{2a^2}. \quad (25)$$

In their analysis of hard sphere solutes, Huang *et al.*⁸ truncated the series expansion for $\tilde{\gamma}$ at first order and identified $c_1/2$ as the Tolman length;²⁸ one can see from Eq. (25) that the coefficient of the $1/a$ term in the series expansion for γ is $c_1/2$ because of the relationship between γ and $\tilde{\gamma}$ given in Eq. (23). Interestingly, the coefficient c_2 cancels from the a^{-2} term in the series expansion of γ ; this fact could be used as justification for truncating the $\tilde{\gamma}$ series at first order.

Even though we obtained γ directly using the mean field approach through Eq. (20), in general it is conceptually simpler to measure $\tilde{\gamma}$ since the solvation free energy is unambiguously defined and can be accurately measured.^{8–14} Since the mean field approach gives us ready access to both γ and $\tilde{\gamma}$, we can assess the accuracy of the route suggested by Eq. (23) to obtain γ indirectly from $\tilde{\gamma}$. In Fig. 5 the surface tension γ from Eq. (20) is plotted against its reconstruction through Eq. (25) for $\delta=0$ and $\delta=4$ Å. The fidelity of the reconstruction is quantitative for $a > 7$ Å in the $\delta=0$ case and $a > 15$ Å in the $\delta=4$ Å case. In order to capture the surface tension behavior below this size, we would need to include higher order terms in the series expansion of Eq. (24). One can also see from Fig. 5 that the second order term, which is only present for nonzero δ , makes the reconstructed surface tension less accurate at small a values but more accurate at large a values. It could be expected that $\delta=4$ would lead to a more accurate reconstruction than $\delta=0$ because it is equal to σ_{sl} and hence accounts for the excluded volume of the solid-liquid interaction on the location of the solid-liquid

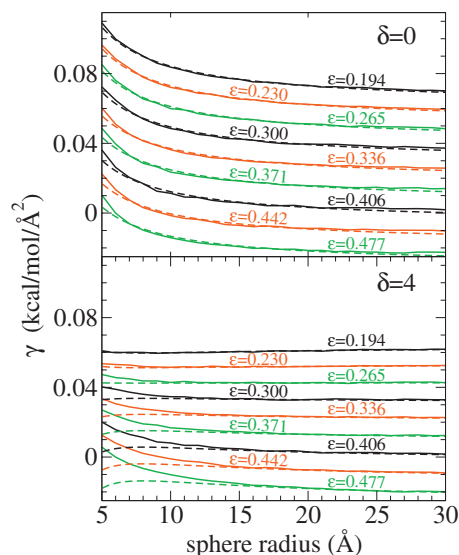


FIG. 5. For a spherical solid-liquid interface, the surface tension γ from Eq. (20) (shown with solid line) is plotted against its reconstruction, Eq. (25) (shown with dashed line), for two different choices of the dividing surface δ (Å). The different curves correspond to different values of the solid-liquid interaction strength ϵ (kcal/mol).

interface; however we see the actual situation is more complicated than this because there is also a dependence on the solid-liquid interaction energy ϵ .

VIII. CONCLUSIONS

The computation of solid-liquid surface tension is challenging, especially for nanoscale interfaces. We demonstrated that great physical insight could be achieved by using a theoretical framework in which the solid was represented as a continuum of uniform density in analogy to Hamaker's treatment of colloidal particles. As a result of this mean field treatment the Hamiltonian of the system was imbued with parametric dependence on the size of the solid object through the integration limits for the solid-liquid interaction energy. Since the solid-liquid surface area is a function of the size of the solid, and the surface tension is the derivative of the system free energy with respect to this surface area, we obtained a simple expression for the surface tension γ of an interface of arbitrary shape. This expression is $\gamma = (\partial G / \partial A)_{NPT} = (\langle \partial U / \partial a \rangle + P \langle \partial V / \partial a \rangle) (dA / da)^{-1}$ where a is the size of the solid object, U is the solid-liquid interaction energy, A is the surface area of the interface, and the angle brackets are understood to be evaluated in the isothermal-isobaric ensemble; equivalently $\gamma = (\partial F / \partial A)_{NVT} = \langle \partial U / \partial a \rangle \times (dA / da)^{-1}$ in the canonical ensemble.

Moreover, our formalism yielded a differential equation relating the surface tension γ to the excess solvation free energy per unit surface area $\tilde{\gamma}$; these quantities converge to a common value for macroscopic interfaces but are distinct on the nanoscale. We explored in detail the relationship between these two quantities for a thin nanoribbon and a solid spherical nanoparticle immersed in liquid using MD simulations. Knowledge of the precise relationship between γ and $\tilde{\gamma}$ is important because most simulation studies report one or the

other but not both. Intriguingly, we showed that assignment of the Tolman length depends on which quantity is analyzed.

In summary, we have formulated an approach to the calculation of solid-liquid surface tension and excess solvation free energy per unit surface area by introducing a size parameter a of the solid object into the system Hamiltonian through a mean field treatment. If desired, information about the actual solid-liquid interface (which, for example, could have defect sites) could be recovered by using algorithms from the literature. The size parameter a can encode for a variety of nanoscale interfaces, for example, spherical (where a is the radius) or ribbonlike (where a is the ribbon width) as considered here, or polyhedral (where a can be the edge length), cylindrical (where a can be the radius), conical (where a can be the cone angle), or of negative curvature such as a spherical or cylindrical cavity.

- ¹F. Leroy, D. J. V. A. dos Santos, and F. Müller-Plathe, *Macromol. Rapid Commun.* **30**, 864 (2009).
- ²B. P. Binks and J. H. Clint, *Langmuir* **18**, 1270 (2002).
- ³L. Schimmele, M. Napiórkowski, and S. Dietrich, *J. Chem. Phys.* **127**, 164715 (2007).
- ⁴A. Amirfazli and A. W. Neumann, *Adv. Colloid Interface Sci.* **110**, 121 (2004).
- ⁵M. P. Allen and D. J. Tildesley, *Computer Simulations of Liquids* (University Press, Oxford, 1992).
- ⁶D. Frenkel and B. Smit, *Understanding Molecular Simulation* (Academic Press, San Diego, 2002).
- ⁷E. Salomons and M. Mareschal *J. Phys.: Condens. Matter* **3**, 3645

- (1991).
- ⁸D. M. Huang, P. L. Geissler, and D. Chandler, *J. Phys. Chem. B* **105**, 6704 (2001).
- ⁹D. M. Huang and D. Chandler, *J. Phys. Chem. B* **106**, 2047 (2002).
- ¹⁰S. Rajamani, T. M. Truskett, and S. Garde, *Proc. Natl. Acad. Sci. U.S.A.* **102**, 9475 (2005).
- ¹¹R. M. Lynden-bell and T. Head-Gordon, *Mol. Phys.* **104**, 3593 (2006).
- ¹²L. R. Pratt and A. Pohorille, *Proc. Natl. Acad. Sci. U.S.A.* **89**, 2995 (1992).
- ¹³K. Lum, D. Chandler, and J. D. Weeks, *J. Phys. Chem. B* **103**, 4570 (1999).
- ¹⁴F. M. Floris, *J. Phys. Chem. B* **109**, 24061 (2005).
- ¹⁵H. C. Hamaker, *Physica (Amsterdam)* **4**, 1058 (1937).
- ¹⁶J. Miyazaki, J. A. Barker, and G. M. Pound, *J. Chem. Phys.* **64**, 3364 (1976).
- ¹⁷L. Onsager, *Chem. Rev. (Washington D.C.)* **13**, 73 (1933).
- ¹⁸R. D. Mountain and D. Thirumalai, *J. Phys. Chem.* **93**, 6975 (1989).
- ¹⁹N. D. Lu, D. A. Kofke, and T. B. Woolf, *J. Comput. Chem.* **25**, 28 (2004).
- ²⁰B. Smit, *J. Chem. Phys.* **96**, 8639 (1992).
- ²¹T. Ingebrigtsen and S. Toxvaerd, *J. Phys. Chem. C* **111**, 8518 (2007).
- ²²W. Shinoda, R. DeVane, and M. L. Klein, *Mol. Simul.* **33**, 27 (2007).
- ²³W. Shinoda, R. DeVane, and M. L. Klein, *Soft Matter* **4**, 2454 (2008).
- ²⁴P. B. Moore and M. L. Klein, "Implementation of a general integration for extended system molecular dynamics," University of Pennsylvania Technical Report, 1997. Available at <http://www.westcenter.usp.edu>.
- ²⁵W. Shinoda and M. Mikami, *J. Comput. Chem.* **24**, 920 (2003).
- ²⁶U. O. M. Vázquez, W. Shinoda, P. B. Moore, C.-c. Chiu, and S. O. Nielsen, *J. Math. Chem.* **45**, 161 (2009).
- ²⁷J. S. Rowlinson and B. Widom, *Molecular Theory of Capillarity* (Dover, Mineola, NY, 2002).
- ²⁸R. C. Tolman, *J. Chem. Phys.* **17**, 333 (1949).